INT. J. REMOTE SENSING, 20 DECEMBER, 2004,
VOL. 25, NO. 24, 5543–5555

Taylor & Francis
Taylor & Francis Group

NOAA/AVHRR satellite detection of Siberian silkmoth outbreaks in eastern Siberia

V. I. KHARUK*†, K. J. RANSON‡, A. G. KOZUHOVSKAYA†, Y. P. KONDAKOV† and I. A. PESTUNOV†

†Sukachev Institute of Forest, Krasnoyarsk, Russia
‡NASA's Goddard Space Flight Center, Code 923, Greenbelt, MD 20771, USA

(*Received 1 November 2000; in final form 13 April 2004*)

Abstract. During 1993–1996, in central Siberia, a silkmoth (*Dendrolimus superans sibiricus* Tschetw.) infestation damaged approximately 700 000 ha of fir, Siberian pine and spruce stands. Temporal (1995–1997) Advanced Very High Resolution Radiometer (AVHRR) images were used for pest outbreak monitoring of this event. Damaged stands were detected, with heavy (50–75% dead and dying trees) plus very heavy (>75%) levels of damage classified. Summer and winter images were used for delineation of the northern border of the region of pest outbreaks. The Siberian taiga insects were classified with respect to their harmfulness to forests, based on the frequency of outbreaks, the size of the damaged territory, and the available food sources based on forest type.

1. Introduction

Siberia is an immense area stretching from the Ural Mountains on the west to the Russian Far East with total territory similar in size to the continental United States. The Siberian forests are an important source/sink of carbon with total carbon storage in western Siberia estimated to be 4300 MT, and in eastern Siberia about 12 500 MT. Estimated annual carbon depositions are 20 and 60 MT y^{-1}, respectively. There are a number of factors that affect carbon balance in the Siberian forests. The most important factors are insect invasions, fires, air pollution, logging, and exploitation of non-renewable natural resources. There is a critical need to know the extent of the forest types in Siberia and those areas affected by natural and anthropogenic change factors.

These Siberian forests are the habitat of many insect species, periodic outbreaks of which cause a decrease in growth increment, forest decline or mortality over vast areas. Pests are among the primary causes that determine forest successions in Siberia (Larsen 1980). Table 1 lists the main *Lepidoptera* species that cause outbreaks in Siberian forests. The reported damaged area varies from 5000 to more than 1 million ha. In table 1, the values of pest danger are categorized as high (I),

*Corresponding author; tel: 7 3912 494453; email: kharuk@ksc.krasn.ru

International Journal of Remote Sensing
ISSN 0143-1161 print/ISSN 1366-5901 online © 2004 Taylor & Francis Ltd
http://www.tandf.co.uk/journals
DOI: 10.1080/01431160410001719858

Table 1. *Lepidoptera* species that cause forest damage within Krasnoyarsk region.

Insect species	Main food source tree species	Maximum outbreak area (000 ha)	Danger level			
			Forest zones			
			South taiga	Mid taiga	Mountain forest	Forest/ steppe
1 *Dendrolimus superans sibiricus* Tschetw.*	fir, pine, larch, spruce	>1000	I		I	I
2 *Lymantria dispar**	larch, broadleaf	300			II	II
3 *Orgyia antiqua*	larch, birch	40			III	
4 *Dasychira abietis*	spruce, fir, pine, larch	1000	III		III	III
5 *Leucoma salicis**	aspen, willow	100	III	III	III	II
6 *Lymantria monacha**	pine, spruce	5				II
7 *Ectropis bistortata**	spruce	400	II		I	
8 *Bupalus piniarius**	pine	50	III			I
9 *Semiothisa signaria**	spruce, fir	10	III		II	
10 *Simiothisa continuaria*	larch	5			II	III
11 *Erranis jacobsoni**	larch	50			II	II
12 *Biston betularius*	birch	50				III
13 *Phalera bucephala*	birch	50	III		III	II
14 *Clostera anastomosis**	aspen, willow	10	III			II
15 *Zeiraphera rufimitrana*	fir	100	III		III	
16 *Coleophera dahurica*	larch	100			III	II
17 *Zeiraphera griseana*	larch	>1000	III	III	III	

*Species which cause forest mortality.

medium (II) and low (III). Pest danger depends on the size of affected territories, level of defoliation, and tree species. Pests that damage evergreen conifers are considered as very harmful (grade I), since conifers are highly sensitive to defoliation and are the source of valuable wood. Less harmful pests are those which feed on broadleaf species and larch since those deciduous tree species can survive after 2–3 complete defoliations in consecutive years. However, insects can also cause extensive damage to deciduous trees planted as field protection forest strips (shelter belts) since they are often growing in extreme conditions.

Table 1 shows that the primary pest of Siberian forests is *Dendrolimus superans sibiricus* Tschetw., or Siberian silkmoth. Outbreaks of this insect can cover several millions of hectares. The silkmoth caterpillars (with size up to 11 cm) feed upon the needles of fir (*Abies sibirica*) and Siberian pine (*Pinus sibirica*), which are the preferred species, larch (*Larix sibirica*) and, at the peak of an outbreak, spruce (*Picea obovata*). In the central Siberia region Siberian silkmoth outbreaks were observed from the southern border (52° N) of the Krasnoyarsk region to 59° N, and from 84° E on the east to 102° E on the west. Table 2 summarizes available data on the Siberian silkmoth outbreak frequency in Krasnoyarsk region. The analysis of ecology, landscapes and the history of outbreaks allow delineating nine main regions of Siberian silkmoth outbreaks (table 2). The regions were ranked by the following criteria.

1. The frequency of pest outbreaks. This varies within a range of 2–10 outbreak events per century. An outbreak frequency range of 10–8 was marked as grade I, a range of 7–5 outbreaks as grade II, and a range of 4–2 as grade III.

Table 2. *Dendrolimus sibiricus* outbreaks in the forests within Krasnoyarsk region.

Region	Forest types	Heights (m asl)	Main forest species	Frequency of outbreaks (years)	Territory of outbreaks	Level of danger
West Siberian Region						
1. Chulim-Ket	southern taiga	150–200	fir, Siberian pine	I	10	I
Mid Siberian Plateau Region						
2. Priangar'e	southern taiga	170–350	fir	I	9	I
3. Prienisey	mountain taiga	200–450	fir	I	7	I
4. Kan-Birusa	subtaiga–forest steppe	200–350	larch	III	6	III
Altai-Sayan Mountain Region						
5. Kan-Agul	subtaiga–forest steppe	350–500	larch, fir, Siberian pine	III	7	III
	black taiga	450–800		II	9	II
6. Kuznetz-Alatau	subtaiga–forest steppe	500–900	larch	I	10	II
7. Sisim-Tuba	black taiga	500–800	fir	II	4	II
8. West Sayan	black taiga	350–900	Siberian pine, fir	III	3	III
9. Usa	subtaiga–forest steppe	700–1200	larch	III	7	III

2. The size of the territory affected (S). Classified as small (grade III, $S < 10\,000$ ha), medium (grade II, $100\,000 > S > 10\,000$ ha) and very large (grade I, $S > 100\,000$ ha).
3. The available 'food source', i.e. tree species. Fir is the most valuable tree type as a food source for Siberian silkmoth and was assumed as level I, Siberian pine as II, and larch as III.

The total sum of these three criteria was calculated and used for ranking the regions. The summed values 3–4 correspond to the highest level of danger (I), 5–6 to the medium (II), and 7–9 to the lowest (III). The latest Siberian silkmoth outbreak was between 1993 and 1996 and was located mainly in region 2 (table 2 and figure 1(5)) located in the mid Krasnoyarsk region (the 'Priangar'e' region). The total area of this outbreak was about 700 000 ha and included $\sim 300\,000$ ha of dead stands located between 57°–59° N latitude and 93°–98° E longitude. The catastrophic scale of this outbreak requires that adequate methods of detection and control be developed.

1.1. *Satellite data analyses*

Satellite data have long been recognized as a valuable tool for locating and monitoring insect outbreaks in forests. Dottavio and Williams (1983) used Landsat multispectral data to delineate the advancing gypsy moth attack on the hardwood forests of Pennsylvania, USA. Their results demonstrated the utility of these 80 m spatial resolution data, but also discussed the vulnerability of Landsat to frequent cloud cover. Nelson (1983) also used Landsat to successfully monitor spruce budworm defoliation. More sophisticated processing techniques were used to obtain high correlation of Thematic Mapper derived green leaf fraction and

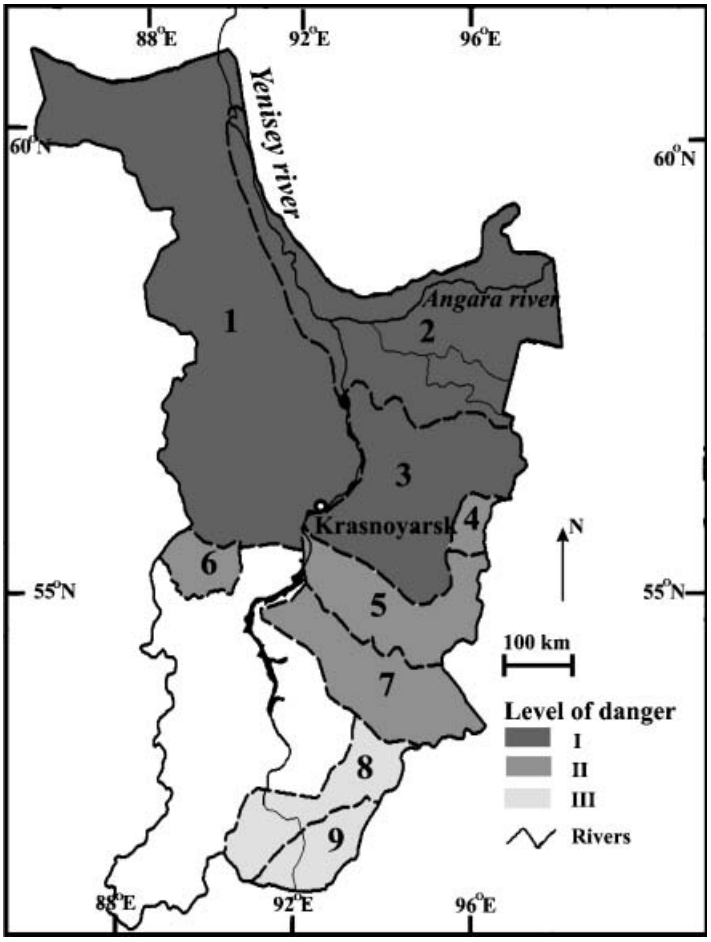

Figure 1. Map of *Dendrolimus sibiricus* outbreak danger in the Krasnoyarsk region. I—high level of danger, II—medium level, III—low level. Arabic numerals correspond to regions described in table 2.

budworm populations (Radeloff *et al.* 1999). Smaller scale satellite data from National Oceanic and Atmospheric Administration (NOAA) Advanced Very High Resolution Radiometer (AVHRR) have been used successfully by Gilli and Gorla (1997) to monitor insect activity in crops. In addition, an initial investigation of NOAA/AVHRR (1.1 km) data for monitoring large-scale pest outbreaks was described in the Russian literature by Kharuk *et al.* (1998). In a later work the validity of the temporal Landsat data for the post-outbreak succession analysis was demonstrated (Kharuk *et al.* 2003a). That analysis includes the area of investigations in this study, and the earlier (1950s) outbreak area.

In this work we analyse in greater detail the potential application of broad-view satellite images (NOAA/AVHRR) for pest monitoring.

2. Study site

The study site is the region of Priangar'e, Siberia, where the latest above-mentioned Siberian silkmoth outbreak took place. The topography of the area

consists of a plateau with low hills. Soils are mainly spodosols (podzols). Climate is continental with cold dry winters and warm moist summers. Annual precipitation is 400–450 mm. Mean annual temperature is $+2.6^{\circ}$C with an absolute minimum of -54°C recorded during December and maximum of $+36^{\circ}$C recorded in July. Vegetative growth period is about 100 days.

Forests cover about 95% of the territory. The dominant species are fir (*Abies sibirica*); other species included are Siberian pine (*Pinus sibirica*) also known locally as Siberian cedar, spruce (*Picea obovata*), pine (*Pinus silvestris*), larch (*Larix sibirica*), aspen (*Populus tremula*), and birch (*Betula pendula*). Stands are of average productivity, corresponding to a III–IV site index of Russian inventory scale (to relate to European scale, the maximum height in 100-year-old stands is 22 m) with a wood stocking density of 200–230 $m^3 ha^{-1}$ and mean age of 135 years.

3. Methods

A time series (1995–1997) of cloud-free AVHRR images from NOAA-12 were used for this analysis. On-ground spatial resolution (pixel size) of the images is about 1.1 km. All AVHRR channels (0.58–0.68 μm; 0.725–1.1 μm; 3.55–3.93 μm, 10.3–11.3 μm, 11.5–12.5 μm) were used in the analysis. The data were received as high-resolution picture transmission (HRPT) images at the AVHRR ground receiving station at the Sukachev Institute of Forest in Krasnoyarsk, Siberia. The IDRISI software was used for image analysis.

A map of insect damage (see figure 5(*b*)) generated by interpretation of airborne false-colour photography (1 : 15 000 scale) acquired in the summer of 1996 was available for comparison with classification results (Anonymous 1996). According to standard Russian forestry photo interpretation procedures, the level of damage was determined by the proportion of dead and dying trees within a given stand. The forest vigour was quantified according to the following scale: 'non-damaged stands' ($<10\%$ of dead and dying trees), 'slightly damaged' (10–25%), 'moderately damaged' (25–50%), 'heavily damaged' (50–75%), and 'very heavily damaged' ($>75\%$ of dead and dying trees). So, alongside affected areas, this map represents non-damaged territories. This scale approximately corresponds to the European scale (European Economic Community (EEC) 1985), also the level of discoloration of leaves is not considered. It should be noted that figure 5(*b*) represents only very heavily and heavily defoliation levels. Along with that map, the false-colour scenes (scale 1 : 200 000 with on-ground resolution 10 m approximately) taken by the KFA-1000 sensor on Russia's 'Resurs-F' satellite in the summer of 1982), and false-colour airborne scenes (scale 1 : 15 000) taken on 16 July 1979 were used in the analysis to identify the pre-outbreak conditions and stands outside the outbreak area. The error matrix was used for the estimation of the accuracy of classification (Richards 1993). The randomly selected points from the AVHRR-derived map were compared with a forest inventory map.

The analysed AVHRR images were of high quality and cloud-free. Consequently, no atmospheric correction was performed. The image processing for detection, localization and mapping damaged forests consisted of several steps. The first one was pre-processing, and included correction of geometric distortion and improvement of the image visual parameters. The correction of geometric distortion was based on establishing a mapping polynomial of the third degree (Richards 1993). Twelve on-ground control points were identified on the reference map and used for estimating polynomial coefficients. Histogram modifications—equalization and saturating linear contrast—were used for improvement of the image visual

parameters. Median and modal filtering were used for removing systematic quantization noise in signal digitizing electronics and noise added to the video signal during transmission (Richards 1993).

The second step includes the feature selection for detection and classification of damaged stands. For the purpose of pest monitoring the most important task is the detection of the initial phases of the forest damage. For this purpose, the following pairs of classes were selected:

- not damaged (background) and slightly damaged stands;
- not damaged (background) and heavily damaged stands;
- slightly and moderately damaged stands;
- slightly and heavily damaged stands.

The Jeffries–Matusita (JM) distance was used as a criterion for classes detection (Richards 1993). It was accepted that the most informative feature (or set of features) was that which has the highest JM value for the pair of classes most difficult to separate. The initial set of features includes values of brightness in the 1, 2, 3 and 5 AVHRR bands and two vegetation indexes—Normalized Difference Vegetation Index (NDVI) and vegetation index: $VI = I_{ir}/I_r$, where I_r, I_{ir} are the values of signals in the first (red) and second (near-infrared) AVHRR bands. The vegetation index values were scaled linearly to the interval [0, 100] for convenient processing.

The training sites on the satellite image were chosen on the base of the reference map. The calculated JM distance for one- and two-dimensional (2D) cases are presented in tables 3 and 4, correspondingly. As evident from those tables, the best discrimination between damage classes for the 1D case are the AVHRR bands 1 and 2, NDVI and VI. For 2D cases pairs (bands 1 and 5, band 1 and VI, and band 2 and VI) provide the best discrimination between classes. An analysis of 3D features was found to be redundant and is not discussed here.

The third step of the image processing included the detection and localization of the damaged sites by image segmentation based on thresholds of the vegetation indices. The damaged sites on the summer images were detected using two thresholds: the first one was used for detection of non-forest areas (such as rivers, bare soil or rock outcrops); the second threshold enables the separation of potential damaged/undamaged sites. For the winter images a third threshold was added for discrimination between snow-covered non-forest territories. The most difficult step in the described procedure of threshold segmentation is detection of non-forest sites

Table 3. The Jeffries–Matusita (JM) distance for the 1D cases. Bg—background (not damaged), Sl—slightly damaged, Md—moderately damaged, Hv—heavily damaged stands.

	Pairs of classes			
Feature	Bg/Sl	Bg/Hv	Hv/Sl	Md/Sl
1 band	2.000	1.548	2.000	2.000
2 band	1.998	2.000	1.964	0.868
3 band	0.346	1.634	0.673	0.156
5 band	1.178	1.865	1.491	0.971
NDVI	2.000	2.000	1.999	1.991
VI	1.999	2.000	2.000	1.975

Table 4. The Jeffries–Matusita (JM) distance for 2D AVHRR cases. Bg—background (non-damaged), Sl—slightly damaged, Md—moderately damaged, Hv—heavily damaged stands.

i class	Bg	Bg	Hv	Md
j class	Sl	Hv	Sl	Sl
Feature combination		JM		
Bands 1 and 2	2.0000	1.4142	2.0000	2.0000
Bands 1 and 3	2.0000	1.4109	2.0000	2.0000
Bands 1 and 5	2.0000	2.0000	2.0000	2.0000
Band 1 and NDVI	2.0000	1.4142	2.0000	2.0000
Band 1 and VI	2.0000	2.0000	2.0000	2.0000
Bands 2 and 3	1.4142	1.4142	1.4142	1.0602
Bands 2 and 5	1.4142	1.4142	1.4142	0.7504
Band 2 and NDVI	2.0000	1.4142	2.0000	2.0000
Band 2 and VI	2.0000	2.0000	2.0000	2.0000
Bands 3 and 5	1.4142	1.4065	1.2943	1.0131
Band 3 and NDVI	1.4142	1.4142	1.4141	1.3788
Band 3 and VI	1.4142	2.0000	2.0000	1.3813
Band 5 and NDVI	1.4142	1.4142	1.4141	1.3145
Band 5 and VI	1.4142	2.0000	2.0000	1.3166
NDVI and VI	2.0000	2.0000	2.0000	2.0000

(e.g. rivers, open south-facing slopes, burned areas) with similar spectral response as damaged forest stands. Localization of such sites is the most difficult problem in the AVHRR image interpretation. On the other hand, those sites were easily discriminated using a geographical information system (GIS) based on maps and other information to exclude these areas from analysis.

The fourth and final step of the image processing included the automatic classification of damaged sites using the FOREL algorithm and construction of the resulting classification map. The FOREL algorithm has only one guided parameter: a threshold R, which is the radius of n-dimensional spheres that describe the classified set in the space of features (Vasiliev 1983).

The diagram of centres of spectral classes distribution which includes all damaged classes is represented in figure 2. It shows the best differentiation observed for heavily + heavy damaged stands, and background based on spectral signatures.

4. Results

The analysed Siberian silkmoth outbreak falls mainly into region 2 of figure 1, which corresponds to the high risk zone. The first signs of outbreak were observed in 1993, the most intensive stand damage was in 1995. Due to a drought (which is an essential factor of pest outbreak) the cloud-free high-quality time-series of NOAA/AVHRR images was obtained. Figure 3 shows the dynamics of pest outbreak for the representative portion of the outbreak area. Two gradations on the figures correspond to the 'heavily' (50–75% of dead and dying trees) and 'very heavily' ($>75\%$ of dead and dying trees) levels of damage. Figure 3(a) shows the beginning of the outbreak, since caterpillars start feeding activity approximately in the middle of May. Figure 3(b) corresponds to the end of June, the month of intensive forest damage. Figure 3(c) summarizes the summer effect of caterpillar damage, since caterpillars stop its activity till the middle of July. During this period the dramatic changes in the size of the affected area take place. For example, within

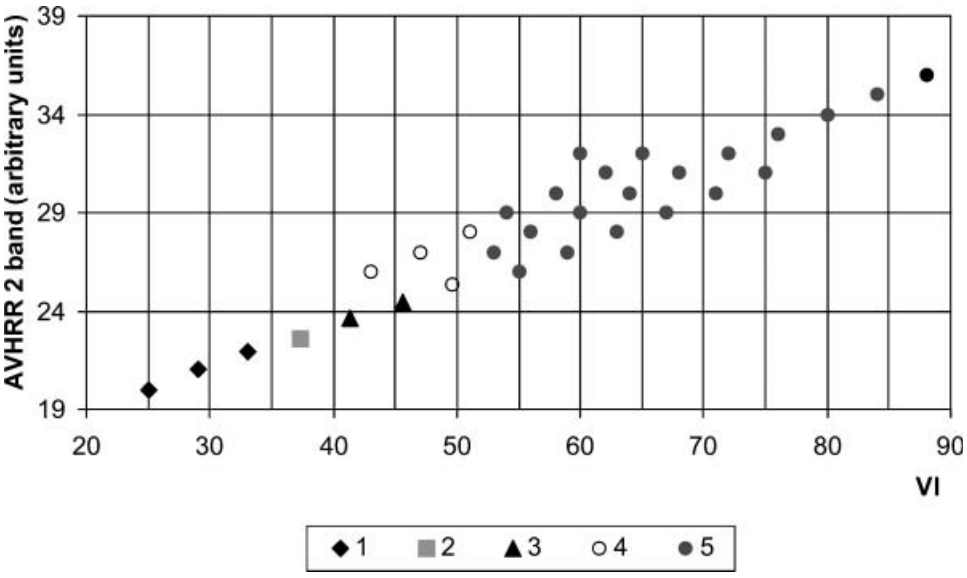

Figure 2. Diagram of the centres of spectral classes distribution. 1—very heavily damaged, 2—heavily damaged, 3—moderately damaged, 4—slightly damaged, 5—background.

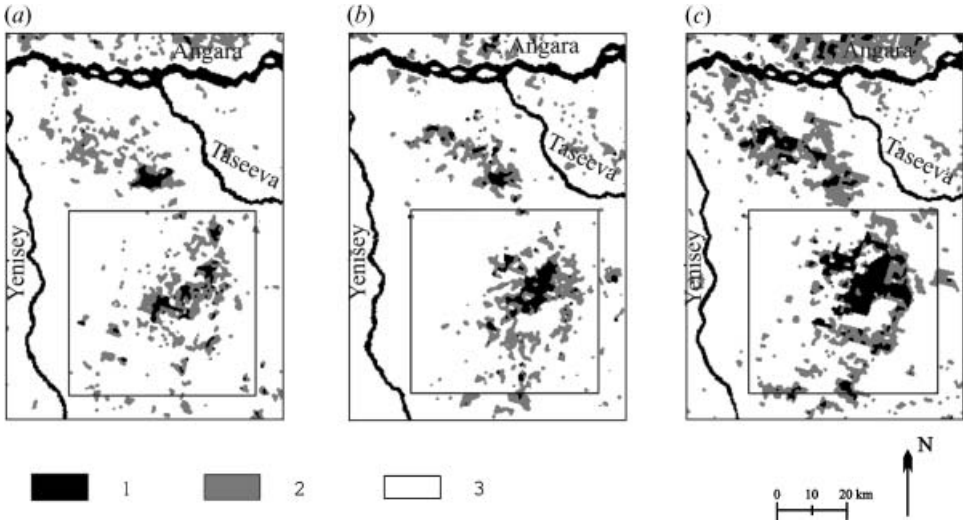

Figure 3. The dynamics of *Dendrolimus sibiricus* outbreak in 1995: (*a*) 7 June, (*b*) 30 June, and (*c*) 16 August. 1—heavily damaged stands, 2—moderately damaged, 3—background.

the window on figure 3 the area of moderately damaged stands increased 1.7 times, and heavily damaged 3.4 times.

The accuracy of the AVHRR-derived damage assessment was estimated for figure 3(*c*), since it reflects the forest's status corresponds to the end of caterpillars' activity. An error analysis shows that the accuracy of classification with detection of the two gradations is poor. Both gradations were joined into one class ('damaged stands'), and an error matrix was calculated (table 5). The user accuracy is

Table 5. An error matrix for the AVHRR-derived classification (figure 3(*c*)).

AVHRR-derived map	Reference map			Producer accuracy (%)	User accuracy (%)
	Background	Damaged	Row total		
Background	82	12	94	61	97
Damaged	53	108	161	90	67
				Overall accuracy	
Column total	135	120	255	74	

satisfactory (67% for the damaged stands and 97% for the background with overall accuracy 74%).

As mentioned above, AVHRR classification procedure using image segmentation enables the detection of two grades of damage: heavily (50–75% of dead and dying trees) and very heavily damaged (>75% of dead and dying trees). The other grades were joined into one class, (i.e. <50% dead and dying trees). The next task was to determine the sensitivity of AVHRR data to lesser damaged forests (i.e. detection of stands with moderate and slight levels of damage). For this purpose a segment of the AVHRR image taken during the phase of maximum damage (16 August 1996, the box on figure 3(*c*)) was analysed. The reference segment (figure 4(*a*)) contains four levels of damage: slight (0–25%), moderate (25–50%), heavy (50–75) and very heavy (>75% of dead and dying trees). Figure 4(*b*) represents the corresponding processed fragment of the AVHRR image. There is some visual similarity between reference (figure 4(*a*)) and classified data (figure 4(*b*)). Also statistical analysis showed that slight and medium levels of damage were not detectable. The probable reasons for these are considered below.

The next important issue is the suitability of data acquired during the winter for monitoring insect damage. Currently regular pest monitoring is based on summer images only, though winter images possess some potential advantages (e.g. lack of the errors caused by broadleaf species and grass communities). To evaluate this problem, late winter images (March and early April 1997) were acquired. In Siberia

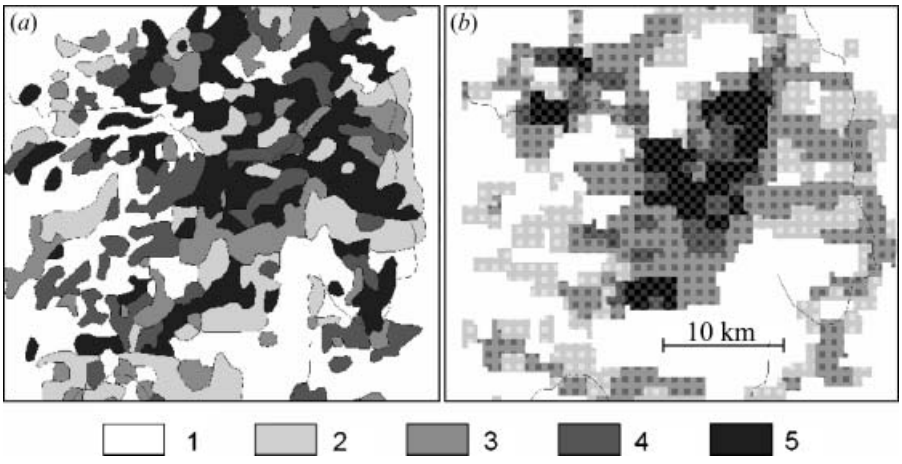

Figure 4. Segments of the reference map (*a*) and classified image (*b*). 1—very heavily damaged, 2—heavily damaged, 3—moderately damaged, 4—slightly damaged, 5—background. The location of the segment shown in figure 3 is shown as a box.

this is a period before the snow melts. In comparison with the deep winter period (December through February), this time period has some advantages, such as higher solar angles, lack of winter frost fogs, and lack of snow on the tree crowns since winds are typical for late winter. On the processed image (figure 5(*a*)) 'dark-needle' taiga (fir + Siberian pine) stands with damaged zones are clearly detectable on the snow background. This classification map represents all the damaged stands present on the reference map (figure 5(*b*)). Moreover, it contains considerable damage areas missed on the reference map. This fact could be due to omission of some damaged stands during the aerial photography flights. An error analysis showed that user accuracy of classification of the damaged stands is 53%, for the background is 91%; an overall accuracy is 82% (table 6). One of the reasons for relatively low accuracy is that part of the area was not covered by aerial survey, so the reference map is initially not complete, and partly, the non-damaged stands could be misclassified as damaged.

The analysed pest outbreak occurs due to a combination of optimal climatic factors (mainly optimal temperature, low precipitation and humidity levels). The outbreaks of similar scale occur with a frequency of every 15–25 years. The investigated outbreak covers the area near the northern known limit of Siberian silkmoth outbreaks. This is an important ecological–geographical and forest management border, which delineates the zone of pest monitoring.

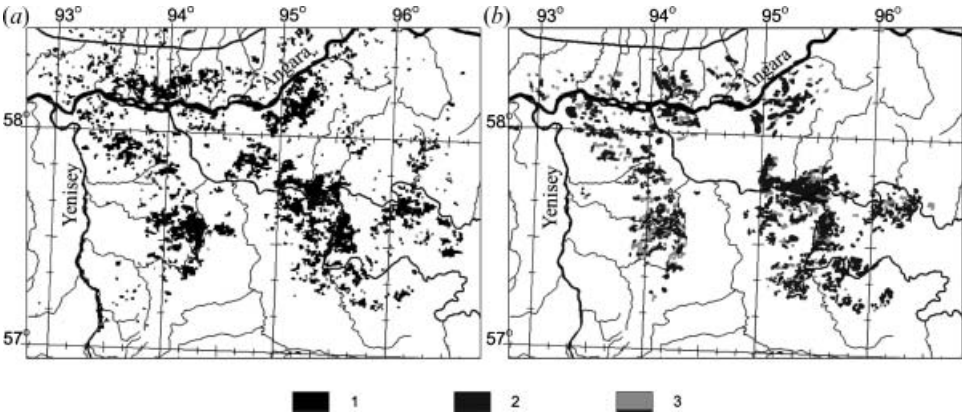

Figure 5. (*a*) Damaged stands (1) appear on the AVHRR image acquired during the winter. (*b*) Reference map. 2, 3—very heavily and heavily damaged stands, respectively. Upper line is the expected limit of insect outbreaks based on an 'index of warmness' with 1400–1600°C values.

Table 6. An error matrix for the AVHRR-derived classification (figure 5(*a*)).

AVHRR-derived map	Reference map			Producer accuracy (%)	User accuracy (%)
	Background	Damaged	Row total		
Background	208	20	228	85	91
Damaged	36	41	77	67	53
				Overall accuracy	
Column total	244	61	305	82	

We consider that the discussed outbreak actually reveals the northern geographical limit of potential pest outbreaks. This border is clearly detectable on both summer and winter images. Since this boundary is controlled by climatic factors, the relevant climatic indexes (e.g. index of warmness, dryness, and precipitation) were analysed. It was found that the northern border could be approximated by a 'warmness index': the annual sum of the positive ($> +10^{\circ}$C) daily temperatures with values in the range of 1400–1600°C (figure 5). This line corresponds to the historical data of Siberian silkmoth outbreaks (figure 1).

5. Discussion

The map of Siberian silkmoth outbreak danger in the western Siberian forests (figure 1) was based mainly on historical data. It is most useful as a general indicator for pest outbreak potential danger. In order to modify this map for operational purposes it is necessary (1) to know the real 'available food sources' for the insect, and (2) to include data of measured weather conditions. The available food sources could be relatively easily estimated since 'dark needle' taiga (fir + Siberian pine) is detectable on the AVHRR images (e.g. Kharuk *et al*. 2003b). Analysis of the insect food sources using GIS technologies (which includes deletion of the territories without appropriate climatic conditions, e.g. high altitude zones) will be useful for the generation of operative maps of potential outbreaks. Climatic data (e.g. indexes of warmness and dryness) could be developed from mid (3.55–3.93 μm) and thermal (10.3–11.3 μm, 11.5–12.5 μm) AVHRR channels. Generally speaking, the potential field of AVHRR data application includes the analysis of ecology and climatic conditions of the given territory, and classification of the territory for pest suitability.

As was shown above, the most useful channels for detection of damaged stands are channels 1 and 2 of NOAA/AVHRR. The first one (0.58–0.68 μm) corresponds to the absorption band of chlorophyll. The signal in the second one (0.725–1.1 μm) is controlled by reflectance/scattering on leaf/needle microstructures, and, indirectly, by Leaf Area Index (LAI) values. So, defoliation causes a decrease of the signal in this band. Defoliation and consequent yellowing of the needles are equivalent to the loss of chlorophyll, and the increased signal level in channel 1 indicates this process.

The sources of the errors in the AVHRR analysis are the following.

1. Forests, as a rule, are non-homogeneous within an AVHRR pixel. Each pixel could include different objects (i.e. different tree species, openings). Nevertheless it should be stressed that the relative homogeneity of the 'black-needle' taiga forest, and the huge geographical area involved make AVHRR data suitable for detection of the damaged territories. It is anticipated that higher resolution from NASA's Terra Moderate-resolution Imaging Spectroradiometer (MODIS) instrument (250 m) will improve results in this regard.
2. The reference map used for analysis of AVHRR images was obtained on the basis of airborne data interpretation. This limits the accuracy assessment of AVHRR classification maps, because: (a) airborne forest inventory is essentially a subjective process ('manual photo interpretation'). As the criterion of the forest damage, the proportion of dead and dying trees was calculated, i.e. trees with high level of damage; whereas NDVI values reflect the continuous scale of defoliation, i.e. allows the qualitative estimate of stand vigour on a more natural basis; and(b) aerial photography for such

vast areas takes much more time. Consequently the dates of satellite-generated and airborne-generated maps do not coincide. This creates some discrepancies between these datasets since the damage level could be significantly changed during a short time as shown in figure 3. For example, at the density of 500–600 silkmoth caterpillars per tree the given stand could be completely defoliated in just 5–10 days. This density was typical of the outbreak in 1995 (with maximal density about 12 000 caterpillars/tree). For comparison, typical populations of Siberian silkmoth caterpillars during the period between outbreaks are only three caterpillars per 10 trees.

3. Even within completely defoliated stands there is chlorophyll containing vegetation, such as non-susceptible forest species (broadleaf species, pine), on-ground vegetation, and bark chlorophyll. It should be noted that bark photosynthesis could be significant for the tree's survival after defoliation (Kharuk *et al.* 1995).
4. The analysis of a temporal sequence of images could be complicated by phenology. For example, figure 3(*a*) corresponds to the very beginning of the vegetative period, when foliage starts to flush and grass communities start to grow. Consequently, the spectral signatures are considerably higher for images taken later (figure 3(*b*), (*c*)).

All of these error sources support the idea that the actual accuracy of satellite-generated maps (figures 3, 4(*b*), 5(*a*) should be higher than was shown by comparison with reference maps.

AVHRR information on the post Siberian silkmoth outbreak situation is very important for estimating the danger of the secondary damage of the weakened forests by bark beetles. One of the most dangerous species is *Monochamus urussovi*, fir bark beetle. Outbreaks of this pest spread over the territory $>100\,000$ ha. Identification of food sources for that species is the priority task of future work.

Satellite data such as NOAA/AVHRR data are very important for an overall system of pest monitoring. NOAA/AVHRR derived products provide foresters with generalized information on the scale of pest outbreak, the food resources available to the insects, and ecological–climatic parameters of the inspected territories. Generally, these data are an adequate tool for detection of large-scale pest outbreaks. On the basis of the results reported here the outbreaks of many insect species listed in table 1 could be detected using AVHRR imagery. The minimal detectable size of outbreak depends on the level of defoliation and homogeneity of the damaged stands. Based on our analysis of these data the expected minimum is 2000–4000 ha. Actually due to lack of the monitoring system (even based on the rough resolution NOAA/AVHRR data) the considered Siberian silkmoth outbreak (1993–1996) was discovered too late, and required expensive pest-suppression methods. NOAA/AVHRR data (or data of its follow-on instrument MODIS) which are acquired daily in Siberia are especially important for monitoring Siberian forests which are of large geographic scale, and because the former system of forest monitoring with aerial and space photography has virtually ceased.

6. Conclusions

1. NOAA/AVHRR summer/winter images are applicable for the analysis of large-scale *Dendrolimus sibiricus* outbreaks with detection of the severe damaged stands. At least two levels of damage could be detected. Detection

of early damage classes was not possible; use of higher resolution Terra MODIS (250 m, 500 m) may improve this situation.

2. A map of the Siberian silkmoth outbreak potential danger zone in the central Siberia forests was generated. It is based on the frequency of outbreaks, the size of the damaged territory, and food source tree species available.
3. The northern border of Siberian silkmoth habitat was delineated. This border could be approximated by an 'index of warmness' values in the range of 1400–1600°C.

Acknowledgments

This work was supported in part by the NASA Office of Earth Science and the Siberian Branch of the Russian Academy of Sciences.

References

ANONYMOUS, 1996, The report on the forest damage caused by Siberian silkmoth. East Siberian State Forestry Enterprise, Krasnoyrsk (in Russian).

DOTTAVIO, C. L., and WILLIAMS, D. L., 1983, Satellite technology—an improved means for monitoring forest insect defoliation. *Journal of Forestry*, **81**, 30–34.

EEC, 1985, *Diagnosis and Classification of New Types of Damage Affecting Forests*, edited by AFZ, BLV-Verlag, Munich (Brussels: Commission of the European Communities).

GILLI, M. P., and GORLA, D. E., 1997, The spatio-temporal pattern of *Delphacodes kuscheli* (*Homoptera: Delphacidae*) abundance in central Argentina. *Bulletin of Entomological Research*, **87**(1), 45–53.

KHARUK, V. I., MIDDLETON, E. M., SPENCER, S. L., ROCK, B. N., and WILLIAMS, D. L., 1995, Aspen bark photosynthesis and its significance to remote sensing and carbon budget estimation of the boreal ecosystem. *Journal of Water, Air and Soil Pollution*, **82**, 483–497.

KHARUK, V. I., ISAEV, A. S., and KOZUKHOVSKAYA, A. G., 1998, NOAA/AVHRR data in pest outbreak monitoring. *Russian Journal of Forestry*, **4**, 20–25 (in Russian).

KHARUK, V. I., RANSON, K. J., KUZ'MICHICHEV, V. V., and IM, S. T., 2003a, Landsat-based analysis of insect outbreaks in southern Siberia. *Canadian Journal of Remote Sensing*, **29**, 286–297.

KHARUK, V. I., RANSON, K. J., BURENINA, T. A., and FEDOTOVA, E. V., 2003b, NOAA/AVHRR data in mapping of Siberian forest landscapes along the Yenisey transect. *International Journal of Remote Sensing*, **24**, 23–37.

LARSEN, J. A., 1980, *The Boreal Ecosystem* (New York: Academic Press).

NELSON, R. N., 1983, Detecting forest canopy change due to insect activity using Landsat MSS. *Photogrammetric Engineering and Remote Sensing*, **49**, 1303–1314.

RADELOFF, V. C., MLADENOFF, D. J., and BOYCE, M. S., 1999, Detecting jack pine budworm defoliation using spectral mixture analysis: separating effects from determinants. *Remote Sensing of Environment*, **69**, 156–169.

RICHARDS, J. A., 1993, *Remote Sensing Digital Image Analysis: An Introduction*, 3rd edn (New York: Springer).

VASILIEV, V. I., 1983, *Recognizing Systems* (Kiev: Naukova Dumka Publishing House) (in Russian).